



Ballistic (n,0) Carbon Nanotube Field Effect Transistors' I-V Characteristics: A Comparison of $n = 3a + 1$ and $n = 3a + 2$

G. R. Karimi*, S. G. Shirazi

Department of Electrical, Faculty of Engineering, Razi University, Kermanshah, Iran

PAPER INFO

Paper history:

Received 31 December 2016

Received in revised form 06 February 2017

Accepted 03 March 2017

Keywords:

Carbon Nanotube
Voltage Effect Transistor
Channel Diameter
Device Performance
Quantum Simulation

ABSTRACT

Due to emergence of serious obstacles to scaling of transistors' dimensions, it has been obviously proved that silicon technology should be replaced by a new one having a high ability to overcome the barriers of scaling to nanometer regime. Among various candidates, carbon nanotube (CNT) field effect transistors are introduced as the most promising devices for substituting the silicon-based technologies. Since the channel of these transistors is made of CNT then its properties, such as chiral vector, have prominent effects on determining the performance of devices. In this paper the CNT diameter impact on tunneling and thermionic emission (TE) currents of a coaxially-gated carbon nanotube field effect transistor (CNTFET) with doped source/drain extensions is investigated. The source/channel/drain of this transistor are a zigzag CNT with (n,0) chirality. The "n" value could be in the form of $n = 3a + 1$ or $n = 3a + 2$. By increasing the "a", the diameter increases while the energy band gap E_G of the CNT decreases; as a result by increasing the "a" value, the on/off current ratio decreases. However, for $n = 3a + 2$ the E_G of a CNT shows a higher value; then at a given "a", for $n = 3a + 1$ the on/off current ratio may decrease due to a lower E_G and hence higher tunneling and TE current. Generally, subthreshold swing improves and threshold voltage increases for a lower diameter device; consequently, the leakage current could diminish. ON-state current and output conductance have higher values for a higher diameter. Also, the difference between E_G and hence the I-V characteristics of the device with $n = 3a + 1$ and $n = 3a + 2$ is negligible for a higher diameter value. All the results are justified based on the energy-position resolved electron density and current spectrums on energy band diagram of the device.

doi: 10.5829/idosi.ije.2017.30.04a.09

NOMENCLATURE

a_{cc}	Carbon-carbon bond length (m)	Σ_D	Drain self-energy matrix
\vec{C}	Chiral vector of CNT	Σ_S	Source self-energy matrix
D_S	Source density of state (eV.m) ⁻¹	Σ_C	Scattering self-energy matrix
D_D	Drain density of state (eV.m) ⁻¹	Greek Symbols	
d	CNT diameter (m)	Γ_D	Drain braodening matrix
e	Electric charge = 1.602×10^{-19} (C)	Γ_S	Source braodening matrix
E	Energy (eV)	η^+	Infinitesimal positive value
E_N	Charge neutral level (eV)	\dagger	Conjugate transpose of a matrix
E_{FS}	Source Fermi level (eV)	Subscripts	
E_{FD}	Drain Fermi Level (eV)	cc	Carbon-carbon bond
F	Fermi-Dirac distribution function	C	Scattering mechanism
G	Retarded Green's function	D	Drain
G^\dagger	Advanced Green's function	F	Fermi level
I	Current (A)	N	Neutrality
T	Transmission probability	S	Source
Z	Position along the tube axis (m)		

*Corresponding Author's Email: ghkarimi@razi.ac.ir (G. R. Karimi)

Please cite this article as: G. R. Karimi, S. G. Shirazi, Ballistic (n,0) Carbon Nanotube Field Effect Transistors' I-V Characteristics: A Comparison of $n = 3a + 1$ and $n = 3a + 2$, International Journal of Engineering (IJE), TRANSACTIONS A: Basics Vol. 30, No. 4, (April 2017) 516-522

1. INTRODUCTION

Exceptional electrical properties of carbon nanotubes (CNTs) [1-3], have made them extensively attractive for future electronics. CNTs are applied to develop different fields of technology [4-8]. Their one-dimensional geometry results in interesting electrical properties. Having longer mean free path and capability of depositing high-k dielectrics constant in field effect devices [2, 3] are some aspects of these properties; as a result, in a nanotube, low bias electron transport can be nearly ballistic across distances of several hundred nanometers.

First demonstration of the CNTFET was in 1998 [9, 10] and up to now extensive improvements have occurred in their structures and performances. These devices, generally, are divided into two types. First fabricated CNTFETs operated like Schottky barrier FET and were called CNT-SBFETs [11, 12]. They can be used as n or p-type devices and consequently are suitable devices for using in complementary MOS (CMOS) systems [13-15]. But, due to the large leakage, the OFF-state current increases. Their operation depends on adjusting the threshold voltage properly. In the second type of CNTFETs, source and drain regions are created by doping extension of the CNT [16, 17] along the channel. These devices are called CNT-MOSFETs and operate like conventional MOSFETs. A CNT-MOSFET improves the ballistic ON-state current of the device at high gate voltages and suppresses the leakage current. For this reason, in this work, we focus on performance of the CNT-MOSFETs and their dependence on the CNT diameter. This device is a coaxially-gated CNTFET with doped source/drain extensions which are created along the channel as is shown in Figure 1(a). The device structure is based on a single-walled CNT. The energy band diagram of the device is shown in Figure 1(b).

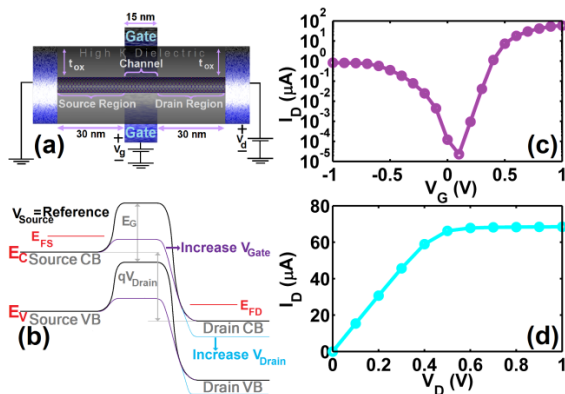


Figure 1. (a) Coaxially-gated CNT-MOSFET structure [18, 19], (b) energy band diagram, (c) transfer $I_D - V_G$ and, (d) output $I_D - V_D$ characteristics of the device

Due to the constant doping level (m^{-1}) considered here, the concentration level does not change with diameter. As a result, by changing the channel's diameter, source/drain Fermi level does not change. A typical $I_D - V_G$ and $I_D - V_D$ characteristics of this device are shown in Figures 1(c) and (d), respectively.

In this paper, the impact of variations in carbon nanotube's diameter on current mechanisms for the device is studied. The changes in performance will be graphically justified using electron distribution function on energy band diagram of the device which is easy to understand. This method also gives an interesting intuition to the readers about electronic operation of any 1D nanowire devices.

2. MODELING

Simulation of electronic devices in nanoscale regime, commonly involved a self-consistent procedure between electrostatic potential and the charge distribution inside the channel [19-22].

When a device is coupled to contacts (electrodes), some charge is transferred into or out of the device, or some electric field lines penetrate into or emerge out of the device. Both effects will yield a self-consistent potential. This potential is called self-consistent because any changes in this potential alter the charge density inside the device. Consequently, the potential is modified by these changes until both charge density and the potential converge to consistent values. To correctly model this process we need to solve two major equations in the simulations. The first one is Poisson equation which determines the self-consistent potential for a given charge density. The other is the transport equation which is solved to obtain the electron density inside the device for any given potential. Since in nanoscale regime the wave-like behavior of electrons become significant than substance behavior, the semi-classical Boltzmann transport equation (BTE) does not verify carrier transportation anymore [19-22]. As a result, a full quantum mechanical transport model, such as the non-equilibrium Green's function (NEGF) approach is necessary. In this method the Schrödinger and Poisson equations should be solved self consistently [20-22]. This paper is devoted to probe the results in detail and justify them by using the electron distribution function of the device on energy band diagram, as well. However, we review the main idea of the simulation approach.

In NEGF method, according to Figure 2, the device is introduced by its Hamiltonian matrix, H , which is connected to the two infinity reservoirs called source and drain. The reservoirs, as is shown in Figure 1(b), are introduced by their Fermi levels E_{FS} and E_{FD} that are determined by the bias voltages applied to reservoirs.

The connection between the active region and source/drain contacts is determined by the self-energy matrices, Σ_S and Σ_D . The scattering process of carrier transportation inside the device is known by Σ_C , the scattering self energy matrix. However, in the ballistic transport consideration, the scattering processes inside the channel are neglected.

The charge density is determined by the integral of local density of states over the energy space.

$$Q(Z) = (-e) \int dE. \text{sgn}[E - E_N(Z)] \{ D_S(E, Z) f(\text{sgn}[E - E_N(Z)](E - E_{FS})) + D_D(E, Z) f(\text{sgn}[E - E_N(Z)](E - E_{FD})) \} \quad (1)$$

where, e is electron charge, $\text{sgn}(E)$ is sign function, $E_{FS(D)}$ is the Fermi level of source (drain), $E_N(Z)$ is the charge neutrality level, and the $D_{S(D)}(E, Z)$ is the local density of states in source (drain) contact which is obtained as follows:

$$D_{S(D)} = G \Gamma G^\dagger \quad (2)$$

In this equation G and G^\dagger are the retarded and advanced Green's functions, respectively. G is given by:

$$G(E) = [(E + i\eta^+)I - H - \Sigma_S - \Sigma_D - \Sigma_C]^{-1} \quad (3)$$

where, H is the device's Hamiltonian and $\Sigma_{S(D)}$ is source (drain) self energy matrix. According to (4):

$$\Gamma_{S(D)} = i(\Sigma_{S(D)} - \Sigma_{S(D)}^\dagger) \quad (4)$$

$\Gamma_{S(D)}$ is the broadening function of source (drain).

After self-consistent procedure between charge density extracted from Schrödinger equation by using the NEGF approach, and the potential obtained from Poisson equation, the self-consistent potential can be inserted into (3) for determining the Green's function until the transmission $T(E)$ inside the device is determined from (5). It should be mentioned that the self-consistent potential is a main part of H matrix which defines the active region of the device.

$$T(E) = \text{trace}(\Gamma_S G \Gamma_D G^\dagger) \quad (5)$$

At the end, the source to drain current can be obtained:

$$I_d = \frac{4e}{h} \int dE T(E) [f(E - E_{FS}) - (E - E_{FD})] \quad (6)$$

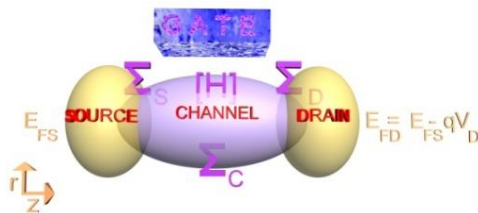


Figure 2. The quantities of the NEGF calculation [19, 23]

3. CARBON NANOTUBE STRUCTURE

The structure of a single-wall carbon nanotube is determined by original hexagonal lattice vector, called the chiral vector. In Figure 3, a graphical representation of chiral vector is shown. It is perpendicular to the axis of tube, T , which is called translational vector.

The chiral vector is a linear combination of the base vectors \vec{a}_1 and \vec{a}_2 [2,3]:

$$\vec{C}_h = n\vec{a}_1 + m\vec{a}_2 \quad (7)$$

where n and m are integer numbers. If the chiral vector is $(n, 0)$ the CNT is called zigzag CNT and when it is (n, n) the CNT is called armchair.

Other forms of CNTs are called chiral. It should be mentioned that n value of semiconducting zigzag CNT and its diameter obey the following equation:

$$d = \frac{n\sqrt{3}a_{cc}}{\pi} \quad (8)$$

where, $a_{cc} = 1.44 \text{ \AA}$ is carbon-carbon bond length in graphene. The channel of a transistor is a semiconductor. For this reason, $(n - m)$ should not be a multiple of 3. So we cannot use (n, n) CNT as a channel because of its metallic behavior. Generally, the energy band gap E_G of a zigzag CNT and its diameter are related to each other inversely [2,3]. However, as is shown in Figure 4, at a constant a value, E_G for $n = 3a + 2$ stands higher while its diameter is higher than $n = 3a + 1$.

4. RESULTS AND DISCUSSION

In order to better understand the current mechanisms, approved tools and resources are used [23-26]. The drain/source current versus the gate voltage (transfer characteristic) of this transistor is shown in Figure 1(c). When a CNT-MOSFET is in a high gate bias the important mechanism in carrier transport is thermionic emission (TE) current. When the gate voltage is high the potential barrier will be low.

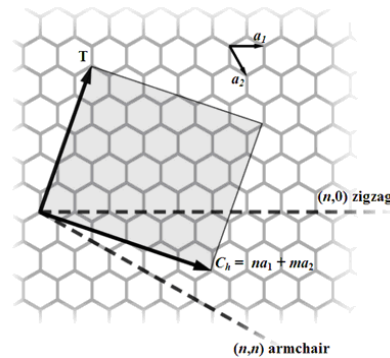


Figure 3. A sheet of graphene and corresponding chiral vector representation

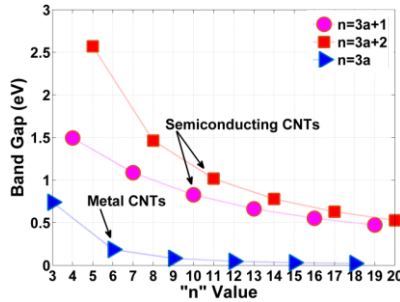


Figure 4. Energy band gap E_G for 3 different groups of zigzag CNTs; $n = 3a + 1$ and $n = 3a + 2$ refer to semiconducting and $n = 3a$ refers to metal CNTs

The source Fermi level E_{FS} has been set as reference. Since the CNT channel is intrinsic and its E_F is $E_G/2$, by applying no gate voltage, at source/channel junction its Fermi level aligns with E_{FS} and height of barrier between them is determined by energy bandgap of channel, E_G . In other words, the barrier height will be equal to E_{FS} from E_C plus $E_G/2$. By increasing the gate voltage, the conduction band E_C and valance band E_V of the channel will drop to a lower energy level and consequently, the E_{FS} could stay above the E_C of channel. Consequently, with respect to energy-position resolved electron (electron density per unit energy (eV) per unit length (nm)) and current (Log of current per unit energy (eV) per unit length (nm)) spectrums in this condition, as is shown in Figures 5(a) and (c), the TE current plays the most important role in carrier transport from source to drain. When the gate voltage of device gradually decreases to lower values, the potential barrier height will become higher and higher. E_{FS} stays at zero; but E_C of channel stays above E_{FS} and due to a growth in potential barrier height, TE current starts decreasing. Since the E_G of channel is constant, E_C and E_V of the channel will rise up simultaneously. This increasing continues until the channel E_V aligns with the source E_C . Thus a quantum well will be created at this junction and the confined states (discrete quantum states) produce a new current mechanism in carrier transport, called band-to-band-tunneling (BTBT) current, as shown in Figures 5(b) and (d). Dominance of tunneling current strongly depends on V_G and E_G of CNT channel. If E_G of channel is high, the tunneling would start at a lower gate bias.

Also, leakage current which includes any current mechanism at zero gate voltage, becomes significant when both the TE and band-to-band tunneling mechanisms have a small value. The leakage current is very important in determining the device performance at the subthreshold region. The thermal component of leakage current is triggered by the electrons movement from source region across the top of the potential barrier. This is due to the lattice temperature which exists in all of the transmission stages.

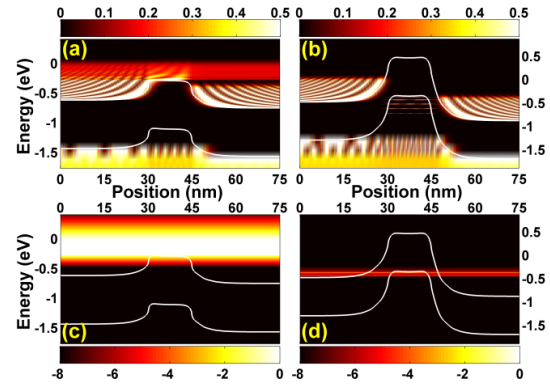


Figure 5. Electron density spectrum at (a) $V_G = 0.8 V$, (b) $V_G = -0.1 V$; corresponding current density spectrum at (c) $V_G = 0.8 V$, and (d) $V_G = -0.1 V$; $V_D = 0.4 V$

In such a situation the difference between Fermi functions of source and drain expands to the higher and lower energies of channel conduction and valance band, respectively [27].

Since the leakage value is very small, i.e. in the order of $10^{-5} \mu A$, it doesn't affect the high current values of the saturation and inverse saturation current (due to BTBT).

For high n values, E_G of channel is small and the channel E_V reaches the source E_C at a higher gate voltage; Hence the minimum current in $I_D - V_G$ characteristics stays at a higher value. $I_D - V_G$ characteristics and subthreshold swing for different diameters are shown in Figures 6(a) and 6(b), respectively.

At first, channels with $n = 3a + 1$ are discussed ($n = 10, 13, 16$ and 19). As mentioned above, by increasing the n value the minimum amount of current increases as well. We can compare the electron distribution function of (13,0) and (19,0) channel at $V_G = 0 V$ to find this fact. It can be seen that drain current at $V_G = 0 V$ increases with n . For $n = 13$, the electron density is significantly lower than $n = 19$ as is shown in Figures 7(a) and (b), respectively.

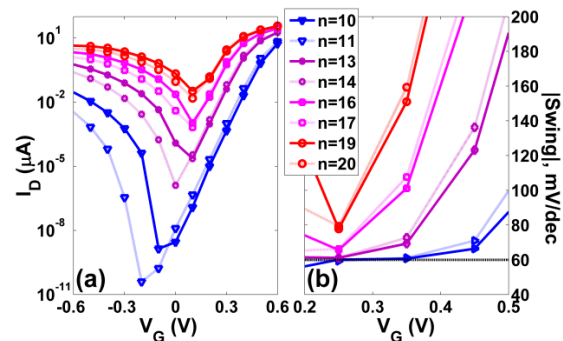


Figure 6. (a) $I_D - V_G$ characteristics, and (b) subthreshold swing; $V_D = 0.4 V$

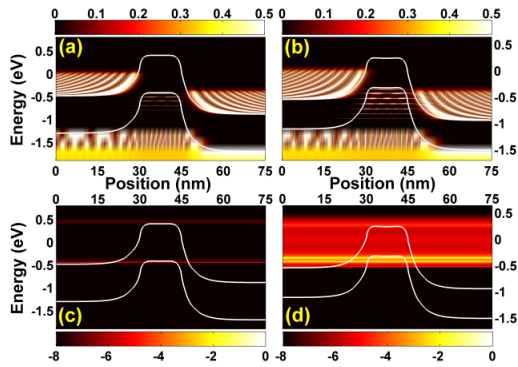


Figure 7. Electron density spectrum for (a) (13,0), (b) (19,0); corresponding current density spectrum for (c) (13,0), and (d) (19,0); $V_G = 0 \text{ V}$, $V_D = 0.4 \text{ V}$

As a result, the OFF-state current is also lower for $n = 13$ than $n = 19$ as is shown in Figures 7(c) and (d), respectively. Increasing the n value causes the E_G of channel to decrease and therefore the tunneling current is strengthened. The BTBT and TE current components are higher for (19,0) than (13,0) at $V_G = 0 \text{ V}$.

The $I_D - V_G$ characteristic for different n values of channel are shown in Figure 8(a) in linear scale to find transconductance g_m , and threshold voltage V_T of the device. As can be seen by increasing the n value, g_m remains almost constant while V_T decreases. The lower V_T is related to lower E_G . One can define the g_m as the slope of the linear regime of $I_D - V_G$ (linear scale) curve and V_T by crossing the slope of the linear regime of $I_D - V_G$ (linear scale) with the voltage axis.

The output conductance g_d of the device (slope of the linear regime of $I_D - V_D$ curve) increases by increasing the n value, as shown in Figure 8(b). If we suppose that $n = 3a + b$ is the case then increasing a decreases E_G , while increasing b (from 1 to 2) increases it, as shown in Figure 4. Lower E_G (higher diameter) improves the ON-state current value at a certain $V_G > V_T$, because channel E_C reaches the E_{FS} at a lower gate field. As a result, the TE occurs at a lower voltage value and current may now reach a higher amount. Then g_d is higher for a higher diameter device.

The same justifications can be used to study the performance of (11,0), (14,0), (17,0) and (20,0) zigzag semiconducting devices ($n = 3a + 2$). Instead, here we compare the two groups, $n = 3a + 1$ and $n = 3a + 2$.

It is obvious that the transistor with $n = 3a + 2$ zigzag semiconducting CNT has lower confinement states at a given $V_G < V_T$ and consequently its OFF-state current I_{OFF} declines, as is shown in Figure 6. Also, as n value rises up from $3a + 1$ to $3a + 2$, the g_m and V_T do not change significantly; and the value of g_d improves a little as is shown in Figures 8(a) and (b), respectively. I_{ON}/I_{OFF} ratio of such devices, when ON-state current I_{ON} is supposed at two groups and two gate voltages in Figure 9.

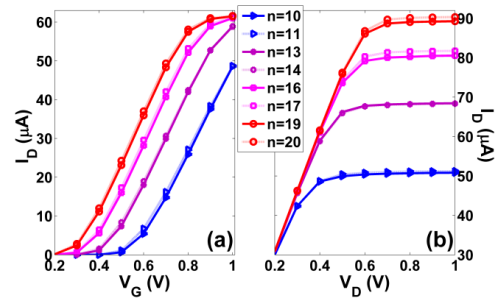


Figure 8. (a) $I_D - V_G$ ($V_D = 0.4 \text{ V}$) and (b) $I_D - V_D$ ($V_G = 0.4 \text{ V}$) characteristics.

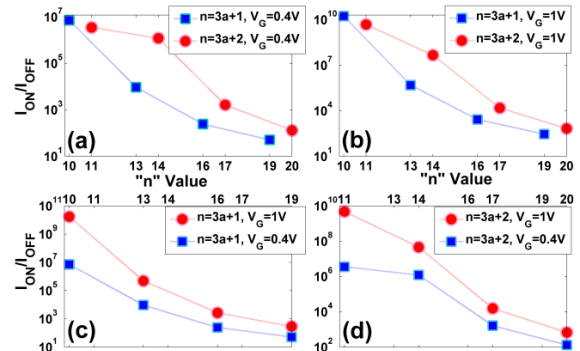


Figure 9. I_{ON}/I_{OFF} for $n = 3a + 1$ and $n = 3a + 2$ at (a) $V_G = 0.4 \text{ V}$, (b) $V_G = 1 \text{ V}$, at $V_G = 1 \text{ V}$ and $V_G = 0.4 \text{ V}$ for (c) $n = 3a + 1$, and (d) $n = 3a + 2$; $V_D = 0.4 \text{ V}$.

Generally, as is shown in Figures 9(a) and (b), by increasing the n value the current ratio diminishes. Also, as discussed before in a higher value of V_G the ON-state current is more due to a lower potential barrier state. Then current ratio is better for a higher V_G , as is shown in Figures 9(c) and (d). As shown in Figure 7, due to a lower E_G of $n = 3a + 1$ than $n = 3a + 2$ at the same a value, BTBT and TE currents could be dominant in carrier transport at $V_G \cong 0$ especially for a higher n value. For these reasons, I_{ON}/I_{OFF} ratio of a device with $n = 3a + 2$ is better than $n = 3a + 1$.

5. CONCLUSION

The role of the CNT diameter on the performance of ($n, 0$) CNT-MOSFET has been studied based on NEGF formalism. The simulation results show that for a large n value (high diameter or low E_G), the tunneling states are prominent at a lower gate voltage. But in a lower n value, the tunneling occurs at a lower gate voltage and OFF-state current is reduced accordingly. By increasing the diameter, the threshold voltage and the output conductance will improve but the I_{ON}/I_{OFF} decreases drastically; however, transconductance of this device is independent of n value. In general, by decreasing the n value the performance of device could improve.

6. REFERENCES

- Iijima, S., "Helical microtubules of graphitic carbon", *Nature*, Vol. 354, No. 6348, (1991), 56-62.
- Saito, R., Dresselhaus, G. and Dresselhaus, M.S., "Physical properties of carbon nanotubes, World scientific, (1998).
- McEuen, P.L., Fuhrer, M.S. and Park, H., "Single-walled carbon nanotube electronics", *IEEE Transactions on Nanotechnology*, Vol. 99, No. 1, (2002), 78-85.
- Afzali, J., Alemipour, Z. and Hesam, M., "High resolution image with multi-wall carbon nanotube atomic force microscopy tip (research note)", *International Journal of Engineering-Transactions C: Aspects*, Vol. 26, No. 6, (2013), 671-679.
- Shafiabadi, M. and Mehrabani, Y.S., "Symmetrical, low-power, and high-speed 1-bit full adder cells using 32nm carbon nanotube field-effect transistors technology (technical note)", *International Journal of Engineering-Transactions A: Basics*, Vol. 28, No. 10, (2015), 1447-1452.
- Yomogida, Y., Tanaka, T., Zhang, M., Yudasaka, M., Wei, X. and Kataura, H., "Industrial-scale separation of high-purity single-chirality single-wall carbon nanotubes for biological imaging", *Nature Communications*, Vol. 7, (2016).
- Shulaker, M.M., Hills, G., Patil, N., Wei, H., Chen, H.-Y., Wong, H.-S.P. and Mitra, S., "Carbon nanotube computer", *Nature*, Vol. 501, No. 7468, (2013), 526-530.
- De Volder, M.F., Tawfick, S.H., Baughman, R.H. and Hart, A.J., "Carbon nanotubes: Present and future commercial applications", *Science*, Vol. 339, No. 6119, (2013), 535-539.
- Tans, S.J., Verschueren, A.R. and Dekker, C., "Room-temperature transistor based on a single carbon nanotube", *Nature*, Vol. 393, No. 6680, (1998), 49-52.
- Martel, R., Schmidt, T., Shea, H., Hertel, T. and Avouris, P., "Single-and multi-wall carbon nanotube field-effect transistors", *Applied Physics Letters*, Vol. 73, No. 17, (1998), 2447-2449.
- Heinze, S., Tersoff, J., Martel, R., Derycke, V., Appenzeller, J. and Avouris, P., "Carbon nanotubes as schottky barrier transistors", *Physical Review Letters*, Vol. 89, No. 10, (2002).
- Appenzeller, J., Knoch, J., Derycke, V., Martel, R., Wind, S. and Avouris, P., "Field-modulated carrier transport in carbon nanotube transistors", *Physical Review Letters*, Vol. 89, No. 12, (2002).
- Ding, L., Zhang, Z., Liang, S., Pei, T., Wang, S., Li, Y., Zhou, W., Liu, J. and Peng, L.-M., "Cmos-based carbon nanotube pass-transistor logic integrated circuits", *Nature Communications*, Vol. 3, (2012), 677-683.
- Wang, C., Chien, J.-C., Takei, K., Takahashi, T., Nah, J., Niknejad, A.M. and Javey, A., "Extremely bendable, high-performance integrated circuits using semiconducting carbon nanotube networks for digital, analog, and radio-frequency applications", *Nano Letters*, Vol. 12, No. 3, (2012), 1527-1533.
- Chen, Z., Appenzeller, J., Lin, Y.-M., Sippel-Oakley, J., Rinzler, A.G., Tang, J., Wind, S.J., Solomon, P.M. and Avouris, P., "An integrated logic circuit assembled on a single carbon nanotube", *Science*, Vol. 311, No. 5768, (2006), 1735-1735.
- Chen, W., "Doped nanomaterials and nanodevices: Luminescence and applications, American Scientific Publishers, (2010).
- Kazaoui, S., Minami, N., Jacquemin, R., Kataura, H. and Achiba, Y., "Amphoteric doping of single-wall carbon-nanotube thin films as probed by optical absorption spectroscopy", *Physical Review B*, Vol. 60, No. 19, (1999).
- Shirazi, S.G. and Mirzakuchaki, S., "Dependence of carbon nanotube field effect transistors performance on doping level of channel at different diameters: On/off current ratio", *Applied Physics Letters*, Vol. 99, No. 26, (2011).
- Shirazi, S.G. and Mirzakuchaki, S., "Performance dependency on doping level of carbon nanotube for ballistic cntfets", *EPL (Europhysics Letters)*, Vol. 103, No. 6, (2013).
- Datta, S., "Nanoscale device modeling: The green's function method", *Superlattices and Microstructures*, Vol. 28, No. 4, (2000), 253-278.
- Datta, S., "Quantum transport: Atom to transistor, Cambridge University Press, (2005).
- Sharifi, M. and Adibi, A., "Semiconductor device simulation by a new method of solving poisson, laplace and schrodinger equations", (2000).
- Guo, J., Koswatta, S.O., Neophytou, N. and Lundstrom, M., "Carbon nanotube field-effect transistors", *International Journal of High Speed Electronics and Systems*, Vol. 16, No. 04, (2006), 897-912.
- Koswatta, S.O., Lundstrom, M.S., Anantram, M. and Nikonov, D.E., "Simulation of phonon-assisted band-to-band tunneling in carbon nanotube field-effect transistors", *Applied Physics Letters*, Vol. 87, No. 25, (2005).
- Koswatta, S.O., Hasan, S., Lundstrom, M.S., Anantram, M. and Nikonov, D.E., "Nonequilibrium green's function treatment of phonon scattering in carbon-nanotube transistors", *IEEE Transactions on Electron Devices*, Vol. 54, No. 9, (2007), 2339-2351.
- Koswatta, S., Guo, J. and Nikonov, D., "Moscent: Code for carbon nanotube transistor simulation", (2006).
- Shirazi, S.G., Karimi, G. and Mirzakuchaki, S., "Temperature dependence of iv characteristics for cnt based pin tfet and nin mosfet", *ECS Journal of Solid State Science and Technology*, Vol. 5, No. 6, (2016), M44-M50.

Ballistic (n,0) Carbon Nanotube Field Effect Transistors' I-V Characteristics: A Comparison of $n = 3a + 1$ and $n = 3a + 2$

G. R. Karimi, S. G. Shirazi

Department of Electrical, Faculty of Engineering, Razi University, Kermanshah, Iran

PAPER INFO

چکیده

Paper history:

Received 31 December 2016

Received in revised form 06 February 2017

Accepted 03 March 2017

Keywords:

Carbon Nanotube

Voltage Effect Transistor

Channel Diameter

Device Performance

Quantum Simulation

در این مقاله اثر قطر نانولوله کربنی نیمه‌هادی با بردار کایرال زیگزاگ بر عملکرد ترانزیستور اثر میدانی نانولوله کربنی در ساختار هم‌محور مورد بررسی قرار می‌گیرد. افزاره با استفاده از شیوه تابع گرین غیرتعادلی شبیه‌سازی می‌گردد. با تغییر قطر، سازوکارهای انتقال حامل در کانال و به دنبال آن عملکرد قطعه دچار تغییر می‌شوند. شاخص کایرالیته نانولوله زیگزاگ به صورت $c = n \times a$ تعریف می‌شود که عدد "n" عددی طبیعی بوده و به دلیل ایجاد ویژگی فلزی در نانولوله نمی‌تواند مضربی از ۳ باشد. بنابراین "n" یکی از دو صورت $n = 3a + 1$ یا $n = 3a + 2$ را خواهد داشت. از آنجا که گرافین در راستای بردار کایرال خود پیچیده شده و نانولوله را تشکیل می‌دهد، با افزایش "n" قطر نانولوله هم زیاد می‌گردد. نتایج شبیه‌سازی نشان می‌دهد افزایش "a" (افزایش قطر یا به‌طور معادل کاهش شکاف باند)، نرخ جریان حالت روشن به خاموش را، به دلیل ایجاد مؤلفه‌های نشتی بیشتر، کاهش خواهد داد. با این حال در یک مقدار ثابت "a"، نانولوله با مقدار $n = 3a + 1$ شکاف باند بیشتری دارد و در نتیجه نرخ جریان بهتری را نشان می‌دهد. در کل، شیب زیرآستانه با کاهش قطر افزاره بهبود می‌یابد؛ ولتاژ آستانه نیز افزایش خواهد یافت و در نتیجه نشتی جریان کاهش می‌یابد. با این حال جریان حالت روشن و هدایت خروجی افزاره در قطرهای بالا چشمگیر است. همچنین افزایش قطر سبب می‌شود اختلاف بین شکاف باند و در نتیجه مشخصات الکتریکی مقادیر $n = 3a + 1$ و $n = 3a + 2$ کاهش یابد. در تمام موارد نتایج با توجه به تابع توزیع الکترون‌ها در دیاگرام باند انرژی افزاره، توجیه می‌گردند.

doi: 10.5829/idosi.ije.2017.30.04a.09